Check for updates

Asian Journal of Control, Vol. 21, No. 4, pp. 1–12, July 2019
Published online in Wiley Online Library (wileyonlinelibrary.com) DOI: 10.1002/asjc.1814

3D MULTI-AGENT FORMATION CONTROL WITH RIGID BODY MANEUVERS

Pengpeng Zhang and Marcio de Queiroz

ABSTRACT

In this paper, we propose a control scheme for the formation maneuvering problem of multi-agent systems where the team of agents can translate and rotate as a virtual rigid body in 3D. Using the single-integrator model, we formulate the basic control law which is comprised of a formation acquisition term, function of the graph rigidity matrix, and a rigid body maneuvering term. The control is dependent on the relative position of agents that are connected in an infinitesimally and minimally rigid framework in addition to the desired rigid body motion of the formation. To facilitate the design of the rigid body maneuver, one agent in the convex hull of the formation serves as the reference point for the rotation component. A simulation study demonstrates the formation controller.

Key Words: Multi-agent system, formation control, rigid body, rigid graph, nonlinear control, Lyapunov stability.

I. INTRODUCTION

A network of autonomous physical agents that jointly executes a task that is unattainable individually is commonly referred to as a multi-agent system. Numerous multi-agent coordination and cooperation problems have been the subject of considerable attention from researchers over the past several years: aggregation, consensus, formation, social foraging, synchronization, containment, distributed averaging/optimization, etc. [11,18–20,22,29,34,39,40]. In this paper, we are primarily concerned with the *formation* problem, which regards the situation where a desired geometric shape in space is assumed and maintained by a team of agents. This paper is devoted to a variant of this problem called formation maneuvering, where the agent team needs to acquire a formation while simultaneously moving as a virtual rigid body with a prescribed (possibly time-varying) velocity. In the most general case, the rigid body motion involves both translational and rotational velocities.

The formation problem is considerably easier to resolve when the global position of the agents can be measured using, for example, GPS. Unfortunately, GPS is unreliable if there is no or limited line of sight between the GPS receiver and satellites. This issue brings up the more challenging problem where the agents have only access to information that is measured locally via onboard sensors, such as an inertial-type navigation system.

When modeling the geometric shape of multi-agent formation, rigid graph theory is a convenient tool since the desired inter-agent distances can be related to the rigidity properties of the graph modeling the formation. Implicitly, this means that agents will not collide while the formation is being acquired. An additional advantage to employing the inter-agent distances as the variables being controlled is that the global positions of the agents are not needed [36]. Rigid graphs were first applied to formation control in [16]. A review of rigid graphs and their use in formation control can be found in [1].

Numerous formation controllers have been proposed which use the inter-agent distances as the controlled variables. When the motion evolves in 2D, formation acquisition (*i.e.*, stabilization to a static formation) controls were presented in [10,15,26,32,36] for the single-integrator motion model, in [7] for the double-integrator model, and in [8] for robotic vehicles with dynamics. For the case of 3D formation acquisition, controllers were given in [31] using single- and double-integrator models. The case of formation acquisition where agents move in two distinct layers (e.g., ground vehicles in the lower layer and air vehicles in the upper layer) was addressed in [33].

With respect to the pure translational maneuvering problem, a 2D formation control was designed in [30] for the single-integrator model when the formation is cycle-free and persistent. 2D translational maneuvering and target interception algorithms were introduced in [9,18] and [6] for the single-integrator

Manuscript received May 19, 2017; revised November 10, 2017; accepted March 2, 2018.

The authors are with the Department of Mechanical and Industrial Engineering, Louisiana State University, Baton Rouge, LA, 70808 USA.

Marcio de Queiroz is the corresponding author (e-mail: mdeque1@lsu.edu).

© 2018 Chinese Automatic Control Society and John Wiley & Sons Australia, Ltd

and double-integrator models, respectively. An iterative learning control law was proposed in [28] that guarantees translational maneuvering in finite time with bounded tracking error. A complex graph Laplacian scheme was presented in [21] for the 2D translational maneuvering problem where the formation scale is determined by the distance between two leader agents. In [35], the 2D translational maneuvering scheme involved a leader with a constant velocity command and followers who track the leader while maintaining the formation shape. The control law consisted of the standard gradient descent formation acquisition term plus an integral term to ensure zero steady-state error with respect to the velocity command. In [38], a class of finite-time consensus tracking controllers were designed for agents with second-order nonlinear dynamics.

Relatively few results exist for the general formation maneuvering problem. A 3D formation maneuvering control law was presented in [37] but without considering the stability of the formation acquisition. In [17], a fuzzy logic-based controller was formulated for uncertain multi-agent systems that accounts for 3D formation rotation with respect to a virtual leader. The rotation maneuver was defined in terms of time-varying inter-agent distances dependent on a rotation matrix. In [14], a 3D consensus-based controller for maneuvering a formation of unmanned air vehicles was proposed using the double-integrator model. A 2D formation maneuvering controller was proposed in [4] for the double-integrator model where the group leader, who has inertial frame information, passes the information to other agents through a directed path in the graph. A limitation of this control is that it becomes unbounded if the desired formation maneuvering velocity is zero. In [27], an optimal control law was designed for finite-time formation tracking where the desired formation and its maneuver were determined by the trajectory of a virtual leader and the homogenous transformation matrix between each agent (follower) and the virtual leader. Recently in [13], a controller was proposed that can steer the entire formation in rotation and/or translation in 3D. The rotation component was specified relative to a body-fixed frame whose origin is at the centroid of the desired formation and needs to be known.

In this manuscript, we introduce an alternative approach to the 3D formation maneuvering problem where the agents' motion is governed by the single-integrator equation. We consider desired formations modeled by an infinitesimally and minimally rigid, undirected framework. To facilitate the specification of the rigid body rotation component, we use the leader-follower concept where the leader serves as the virtual axis of rotation. The graph that represents the desired formation is built with the leader agent in the convex hull of the followers so that the axis can capture pure rotations (*i.e.*, decoupled from pure translations). The control is based on the graph rigidity matrix, and exploits the special structure of this matrix to disassociate the formation acquisition stability analysis from the formation maneuvering analysis. Using Lyapunov-based arguments, we show that the proposed control ensures exponential formation acquisition and asymptotic convergence of the agent velocities to the desired rigid body maneuvering velocity. The contributions of this work are three-fold: (i) the resulting control law has a simple and intuitive structure, consisting of a formation acquisition component plus the rigid body motion component; (ii) the control law only depends on the relative positions of agents that are connected in the formation graph; *i.e.*, the global positions of the agents are not required; and (iii) the formation maneuvering component can be designed to create any rigid body motion. It should be noted that since global positions are not used, the rigid body motion of the formation is relative to the position and orientation of the formation at the time it is acquired.

II. BACKGROUND MATERIAL

An undirected graph (or simply a graph) G is represented by the pair (V, E) where $V = \{1, 2, \dots, n\}$ is a non-empty finite set of vertices and $E = \{(i,j) : i,j \in V, i \neq j\}$ is a non-empty finite set of *undirected* edges in the sense that there is no distinction between (i,j) and (j,i). We let $a \in \{1, \dots, n(n-1)/2\}$ denote the total number of edges in E. The set of neighbors of vertex $i \in V$ is given by

$$N_i(E) = \{j \in V \mid (i,j) \in E\}. \tag{1}$$

If $q_i \in \mathbb{R}^3$ is the coordinate of vertex i, then a framework F is defined as the pair (G, q) where $q = \left[q_1, \dots, q_n\right] \in \mathbb{R}^{3n}$.

Based on any ordering of edges, the edge function $\beta : \mathbb{R}^{3n} \to \mathbb{R}^a$ is defined as

$$\beta(q) = \left[\dots, \left\|q_i - q_j\right\|^2, \dots\right], \ (i,j) \in E \tag{2}$$

such that its kth component, $\left\|q_i - q_j\right\|^2$, relates to the kth edge of E connecting the ith and jth vertices. The rigidity matrix $R : \mathbb{R}^{3n} \to \mathbb{R}^{a \times 3n}$ is given by

$$R(q) = \frac{1}{2}\frac{\partial \beta(q)}{\partial q}, \tag{3}$$

where we have that $\operatorname{rank}\left[R(q)\right] \leq 3n - 6$ [2].

© 2018 Chinese Automatic Control Society and John Wiley & Sons Australia, Ltd

An isometry of $\mathbb{R}^3$ is a map $\mathcal{T} : \mathbb{R}^3 \to \mathbb{R}^3$ satisfying [23]

$$\|w - z\| = \|\mathcal{T}(w) - \mathcal{T}(z)\|, \quad \forall w, z \in \mathbb{R}^3. \tag{4}$$

This map includes rotations and translations of the vector $w - z$. Two frameworks are *isomorphic* in $\mathbb{R}^3$ if they are correlated via an isometry in $\mathbb{R}^3$. In this paper, we will represent the collection of all frameworks that are isomorphic to $F = (G, q)$ where $G = (V, E)$ by Iso (F). This set is formally defined as follows:

$$\text{Iso}(F) := \left\{ (G, \bar{q}) \mid \left\| \bar{q}_i - \bar{q}_j \right\| = \left\| T(q_i) - T(q_j) \right\|, \forall i, j \in V \right\}. \tag{5}$$

It is important to point out that (2) is invariant under isomorphic motions of the framework [26].

Frameworks (G, q) and $(G, \hat{q})$ are equivalent if $\beta(q) = \beta(\hat{q})$, and are congruent if $\left\| q_i - q_j \right\| = \left\| \hat{q}_i - \hat{q}_j \right\|$, $\forall i, j \in V$ [24]. The necessary and sufficient condition for a framework (G, q), where $n > 3$ and the affine span of q is all of $\mathbb{R}^3$ [12], to be infinitesimally rigid (IR) is that $\text{rank}\left[R(q)\right] = 3n - 6$ [23]. An IR framework is said to be minimally rigid (MR) if and only if $a = 3n - 6$ [1]. If the IR frameworks (G, q) and $(G, \hat{q})$ are equivalent but not congruent, then they are referred to as *ambiguous*[1]. The notation Amb(F) will be used here to represent the collection of all frameworks that are ambiguous to the IR framework F. The set Amb(F) is defined as

$$\text{Amb}(F) := \left\{ (G, \bar{q}) \mid \left\| \bar{q}_i - \bar{q}_j \right\| = \left\| T(q_i) - T(q_j) \right\|, \forall (i, j) \in E \cap \left\| \bar{q}_i - \bar{q}_j \right\| \neq \left\| T(q_i) - T(q_j) \right\|, \exists\, i, j \in V \right\}. \tag{6}$$

All frameworks in Amb(F) are also assumed to be IR. According to [1] and theorem 3 of [3], this assumption holds almost everywhere; therefore, it is not restrictive.

The following metric will be used in the paper:

$$\text{dist}(v, \mathcal{A}) = \inf_{x \in \mathcal{A}} \|v - x\| \tag{7}$$

for points $v, x \in \mathbb{R}^3$ and set $\mathcal{A}$. Given $b, c \in \mathbb{R}^3$, we have that

$$b \times c = S(b)c, \tag{8}$$

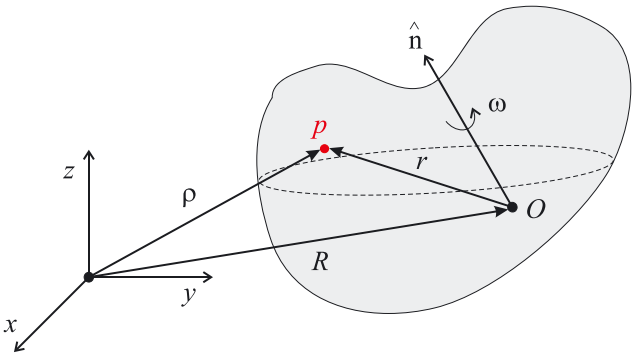

Fig. 1. Rigid body kinematics. [Color figure can be viewed at wileyonlinelibrary.com]

where S is the following skew-symmetric matrix

$$S(b) = \begin{bmatrix} 0 & -b_3 & b_2 \\ b_3 & 0 & -b_1 \\ -b_2 & b_1 & 0 \end{bmatrix}. \tag{9}$$

Finally, we define what is meant by rigid body translation and rotation in this work. A rigid body is said to be in *translation* if all points forming the body move along parallel paths (straight or curvilinear) [5]. A rigid body is said to be in *rotation* if all points move in parallel planes along circles centered on a same axis that *intersects* the body [5]. Note that if the axis of rotation does not intersect the rigid body, the motion is usually called a revolution or orbit. This type of motion (in fact, any type of rigid body motion) can be decomposed into a translation superimposed on a rotation. That is, the above definitions allow one to *decouple* pure translation from pure rotation, thus facilitating the subsequent specification of the desired formation maneuver and the control analysis. Recall from rigid body kinematics that given body-fixed points p and O (see Fig. 1), the following relationship holds

$$\dot{\rho} = \dot{R} + \omega \times r, \tag{10}$$

where $\omega \in \mathbb{R}^3$ denotes the angular velocity of the rigid body about an arbitrary axis n̂ passing through point O and $\{x, y, z\}$ is an inertial coordinate frame.

III. PROBLEM DESCRIPTION

We assume a multi-agent system governed by the following motion equation

$$\dot{q}_i = u_i, \; i = 1, \ldots, n, \tag{11}$$

© 2018 Chinese Automatic Control Society and John Wiley & Sons Australia, Ltd

where $q_i = [x_i, y_i, z_i] \in \mathbb{R}^3$ is the position of the ith agent relative to some inertial coordinate frame and $u_i \in \mathbb{R}^3$ is the corresponding velocity-level control input.

The agents' desired formation is modeled by framework $F^d = (G^d, q^d)$ where $G^d = \left(V^d, E^d\right)$, $\dim(V^d) = n$, $\dim(E^d) = a$, and $q^d = \left[q_1^d, \ldots, q_n^d\right]$. The fixed desired distance separating the ith and jth agents is therefore

$$d_{ij} = \left\| q_i^d - q_j^d \right\| > 0, \quad i,j \in V^d. \tag{12}$$

The agents' actual formation is modeled by $F(t) = \left(G^d, q(t)\right)$ where $q = \left[q_1, \ldots, q_n\right]$. We assume that the ith agent can only measure its relative position to neighboring agents, *i.e.*, $\forall j \in N_i\left(E^d\right)$. In other words, only $q_i - q_j$, $\forall\,(i,j) \in E^d$ is available to the control law

This paper will focus on the formation maneuvering problem for the multi-agent system. The control objective for this problem is twofold and can be stated as follows. Design $u_i = u_i(q_i - q_j, d_{ij}, t)$, $\forall i \in V^d$ and $\forall j \in N_i\left(E^d\right)$ such that:

Objective 1.

$$F(t) \to \mathrm{Iso}\left(F^d\right) \text{ as } t \to \infty. \tag{13}$$

Objective 2.

$$\dot{q}_i(t) - v_{mi}(t) \to 0 \text{ as } t \to \infty,\ \forall i \in V^d, \tag{14}$$

where $v_{mi} \in \mathbb{R}^3$ is the desired rigid body maneuvering velocity for the ith agent.

The desired velocity in (14) is assumed to be known by the ith agent, and will have translation and rotation components to be specified later. To enable the virtual rigid body made up by the multi-agent formation to perform rotations, we assign the nth agent (without lost of generality) to be the *leader* agent with the other agents being *followers*. This assignment is for the sole purpose of one agent serving as a reference point for the axis of rotation of the virtual rigid body (*i.e.*, point O in Fig. 1). To this end, the leader needs to be enveloped by the followers so that the axis of rotation is inside the virtual rigid body. Therefore, F^d should be constructed to the satisfy the following conditions:

1. Be IR and MR.
2. $q_n^d \in \mathrm{conv}\left\{q_1^d, \ldots, q_{n-1}^d\right\}$ where $\mathrm{conv}\{\cdot\}$ denotes the convex hull.
3. All followers should have an edge to the leader, *i.e.*, $n \in N_i\left(E^d\right)$ for all $i \in V$.

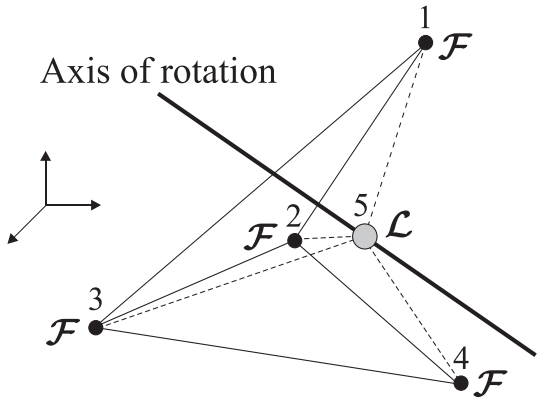

Fig. 2. Example of the construction of F^d: A tetrahedron formation where $\mathcal{L}$ stands for leader and $\mathcal{F}$ for follower. The axis of rotation passes through the leader, which is inside the tetrahedron. Since $n = 5$, we need $3n - 6 = 9$ for the framework to be minimally rigid. The solid lines indicate edges that form the faces of the tetrahedron while the dashed lines are edges in its interior. Notice that edge $(1,4)$ is not necessary.

An example of F^d is illustrated by the 3D formation in Fig. 2 where the leader is located in the interior of the tetrahedron.

Remark 1. The association of a leader agent (instead of a *virtual* leader) with the axis of rotation is done for convenience (not necessity) since a) the leader's relative position to the followers can be measured according to the above Condition 3, and b) it will not have to undergo any rotation. Note that if one uses a virtual leader, its location would have to be known in order to calculate its relative position to the agents (see (10)). This in turn would require extra measurements and/or calculations.

IV. FORMATION MANEUVERING CONTROLLER

The relative position of agents i and j is given by

$$\tilde{q}_{ij} = q_i - q_j, \tag{15}$$

while the corresponding distance error is

$$e_{ij} = \left\| \tilde{q}_{ij} \right\| - d_{ij}. \tag{16}$$

Using (16) and (11), we can calculate the open-loop, inter-agent distance error dynamics to be

$$\dot{e}_{ij} = \frac{d}{dt}\left(\sqrt{\tilde{q}_{ij}^{\top}\tilde{q}_{ij}}\right) = \frac{\tilde{q}_{ij}^{\top}\left(v_i - v_j\right)}{e_{ij} + d_{ij}}. \tag{17}$$

© 2018 Chinese Automatic Control Society and John Wiley & Sons Australia, Ltd

We introduce the function

$$\mathcal{V}_{ij} = \frac{1}{4}\sigma_{ij}^2, \quad (i,j) \in E^d. \tag{18}$$

where

$$\sigma_{ij} = \left\|\tilde{q}_{ij}\right\|^2 - d_{ij}^2 \tag{19}$$

is an alternative error variable. Using (16), it quite simple to verify that (19) can be expressed as

$$\sigma_{ij} = e_{ij}\left(\left\|\tilde{q}_{ij}\right\| + d_{ij}\right) = e_{ij}\left(e_{ij} + 2d_{ij}\right), \tag{20}$$

which indicates that $\sigma_{ij} = 0$ if and only if $e_{ij} = 0$.

Consider the Lyapunov function candidate

$$\mathcal{V}(e) = \sum_{(i,j)\in E^d} \mathcal{V}_{ij}, \tag{21}$$

where $e = \left[\ldots, e_{ij}, \ldots\right] \in \mathbb{R}^a$ is arranged in the same manner as (2). This function is positive definite with respect to e due to (20). The time derivative of (21) is given by

$$\dot{\mathcal{V}} = \sum_{(i,j)\in E^d} e_{ij}\left(e_{ij} + 2d_{ij}\right)\tilde{q}_{ij}^{\top}\left(v_i - v_j\right), \tag{22}$$

where (17) was employed. By use of (3) and (20), the preceding equation can be conveniently expressed as

$$\dot{\mathcal{V}} = \sigma^{\top} R(q) u, \tag{23}$$

where $u = \left[u_1, \ldots, u_n\right] \in \mathbb{R}^{3n}$ and $\sigma = \left[\ldots, \sigma_{ij}, \ldots\right] \in \mathbb{R}^a$, $(i,j) \in E^d$ with terms arranged as in (2). The benefit of (23) is that it naturally lends itself to Lyapunov-based design and analysis.

For convenience, we reproduce the following lemmas from [7] that will be invoked in our main result. The first one formalizes the intuitive notion that infinitesimal rigidity is preserved under small displacements of the framework. The second one relates this result to the level sets of the Lyapunov function candidate (21).

Lemma 1 ([7])**.** Given frameworks $F = (G, q)$ and $\hat{F} = (G, \hat{q})$ with graph $G = (V, E)$ and the function

$$\Lambda(\hat{F}, F) = \sum\left(\left\|\hat{q}_i - \hat{q}_j\right\| - \left\|q_i - q_j\right\|\right)^2, \ (i,j) \in E, \tag{24}$$

if F is IR and $\Lambda(\hat{F}, F) \leq \delta$ for sufficiently small $\delta > 0$, then $\hat{F}$ is also IR.

Lemma 2 ([7])**.** For constants $c, \delta \geq 0$, the level set $\mathcal{V}(e) \leq c$ is equivalent to $\Lambda\left(F, F^d\right) \leq \delta$ where Λ and $\mathcal{V}$ were given in (24) and (21).

The following theorem introduces our formation maneuvering controller and the stability properties of the closed-loop system.

Theorem 1. Consider the formation $F(t) = \left(G^d, q(t)\right)$ with target formation $F^d = (G^d, q^d)$ and the sets

$$\begin{aligned}\Theta_1 &= \left\{e \in \mathbb{R}^a \mid \Lambda(F, F^d) \leq \delta\right\},\\ \Theta_2 &= \left\{e \in \mathbb{R}^a \mid \operatorname{dist}(q, \operatorname{Iso}(F^d)) < \operatorname{dist}(q, \operatorname{Amb}(F^d))\right\},\end{aligned} \tag{25}$$

where the constant $\delta > 0$ is sufficiently small. If the system initial conditions satisfy $e(0) \in \Theta_1 \cap \Theta_2$, then the control

$$u = -k_s R^{\top}(q)\sigma + v_m, \tag{26}$$

where $k_s > 0$ is a control gain, $v_m = \left[v_{m1}, \ldots, v_{mn}\right] \in \mathbb{R}^{3n}$ is the composite rigid body maneuvering velocity vector whose elements are specified by

$$v_{mi} = v_0 + \omega_0 \times \tilde{q}_{in}, \quad \forall i \in V^d, \tag{27}$$

$v_0(t) \in \mathbb{R}^3$ denotes the desired translation velocity for the formation, $\omega_0(t) \in \mathbb{R}^3$ is the desired angular velocity for the formation, and $\tilde{q}_{in}$ is the relative position between agent i and the leader, renders $e = 0$ exponentially stable and solves the formation maneuvering problem.

Proof 1. It is easy to see that since F^d is MR, then $F(t)$ is MR for all $t \geq 0$ given that the two framework have the same edge set. Now, using (26) in (23) gives

$$\dot{\mathcal{V}} = -k_s \sigma^{\top} R(q) R^{\top}(q) \sigma + \sigma^{\top} R(q) v_m. \tag{28}$$

We will focus first on the second term on the right-hand side of (28) and show that $R(q) v_m = 0$. It follows from (3) that each rigidity matrix row is given by

$$\left[0 \ldots 0, \ \left(q_i - q_j\right)^{\top}, 0 \ldots 0, \ \left(q_j - q_i\right)^{\top}, \ 0 \ \ldots \ 0\right]. \tag{29}$$

Therefore, multiplying each $1\times 3n$ row of $R(q)$ by the $3n\times 1$ vector v_m gives

$$\begin{aligned}&\left(q_i - q_j\right)^{\top}\left(v_0 + \omega_0 \times (q_i - q_n)\right)\\ &\quad + \left(q_j - q_i\right)^{\top}\left(v_0 + \omega_0 \times (q_j - q_n)\right)\\ &= \left(q_i - q_j\right)^{\top}\left(\omega_0 \times q_i - \omega_0 \times q_n\right)\\ &\quad - \left(q_i - q_j\right)^{\top}\left(\omega_0 \times q_j - \omega_0 \times q_n\right)\\ &= \left(q_i - q_j\right)^{\top}\left(\omega_0 \times \left(q_i - q_j\right)\right)\\ &= \left(q_i - q_j\right)^{\top} S(\omega_0)\left(q_i - q_j\right) = 0,\end{aligned} \tag{30}$$

© 2018 Chinese Automatic Control Society and John Wiley & Sons Australia, Ltd

where (9) and (15) were used.

From Lemma 1 and the fact that F^d is IR, $F(t)$ is IR for $e(t) \in \Theta_1 \cap \Theta_2$. This implies that $R(q)$ has full row rank for $e(t) \in \Theta_1 \cap \Theta_2$. Given that $\text{rank}\left[R(q)\,R^\top(q)\right] = \text{rank}\left[R(q)\right]$, we have that $R(q)\,R^\top(q)$ is nonsingular for $e(t) \in \Theta_1 \cap \Theta_2$ and as a result

$$\dot{\mathcal{V}} \leq -k_s \lambda_{\min}\left(RR^\top\right)\sigma^\top\sigma = -4k_s\lambda_{\min}\left(RR^\top\right)\mathcal{V} \quad \text{for} \quad e(t) \in \Theta_1 \cap \Theta_2, \tag{31}$$

where $\lambda_{\min}(\cdot)$ is the minimum eigenvalue and (18) and (21) were applied. The above inequality indicates that $\dot{\mathcal{V}}(t) \leq 0$ for all $t \geq 0$, which means $\mathcal{V}(t)$ is constant or decreasing for all time. Therefore, given that $e(t) \in \Theta_1$ is tantamount to $e(t) \in \left\{e \in \mathbb{R}^{3n} \mid \mathcal{V}(e) \leq c\right\}$ according to Lemma 2, a sufficient condition for (31) is

$$\dot{\mathcal{V}} \leq -4k_s\lambda_{\min}\left(RR^\top\right)\mathcal{V} \quad \text{for} \quad e(0) \in \Theta_1 \cap \Theta_2. \tag{32}$$

It follows from (32) that $e = 0$ is exponentially stable for $e(0) \in \Theta_1 \cap \Theta_2$ [25].

The exponential stability of $e = 0$ infers one of two possible occurrences: $F(t) \to \text{Iso}\left(F^d\right)$ or $F(t) \to \text{Amb}\left(F^d\right)$ as $t \to \infty$. Due to $e(0) \in \Theta_1 \cap \Theta_2$, we know from (25) that

$$\text{dist}(q(0), \text{Iso}(F^d(0))) < \text{dist}(q(0), \text{Amb}(F^d(0))). \tag{33}$$

Given this condition, the energy function (21) would necessarily have to grow for a certain time interval for $F(t) \to \text{Amb}\left(F^d\right)$ as $t \to \infty$ to occur. This is however contradictory to the fact that $\mathcal{V}(t)$ is constant or decreasing for all time. Thus, we conclude that $F(t) \to \text{Iso}\left(F^d\right)$ as $t \to \infty$ for $e(0) \in \Theta_1 \cap \Theta_2$.

Lastly, it is obvious from (20) that $\sigma \to 0$ as $e \to 0$. Since we already know e is bounded, (16) can be used to claim $\tilde{q}$ is bounded. It then follows that $R(q)$ is bounded and

$$u \to v_m \quad \text{as} \quad e \to 0 \tag{34}$$

from (26). Given that $e(t) \to 0$ as $t \to \infty$, we can use (34) and (11) to show that $\dot{q}_i(t) - v_{mi}(t) \to 0$ as $t \to \infty, \forall i \in V^d$.

Remark 2. The control law (26) has two clearly-defined components: the component $-kR^\top(q)\sigma$ guarantees formation acquisition while the component v_m is responsible for rigid body maneuvers of the whole formation. Note that the latter term is not purely open-loop in nature since it depends on feedback of $\tilde{q}_{in}$. That is, it is not based on constant, steady-state values as in [13].

Remark 3. Expressing the control algorithm element-wise yields

$$u_i = -k_s \sum_{j \in N_i(E^d)} \tilde{q}_{ij}\sigma_{ij} + v_0 + \omega_0 \times \tilde{q}_{in}, \quad \forall i \in V^d. \tag{35}$$

From this expression, we can see that the control for the ith agent is only dependent on the relative positions of neighboring agents, which can be accomplished with onboard sensors, and v_0 and ω_0. Knowledge of v_0 and ω_0 is not a restrictive requirement since for many applications they are predefined and can be stored on the agent's onboard computer prior to deployment. That is, v_0 and ω_0 can be treated in the same way as F^d. For cases where these velocities are modified on-line due to changes in the mission specifications, their updated values would have to be transmitted to each agent by the leader or a central command.

V. SIMULATION RESULTS

The performance of the formation maneuvering controller defined by (26) and (27) was illustrated via two computer simulations.

Simulation 1. In this simulation, we considered nine agents with the desired formation F^d being the cube

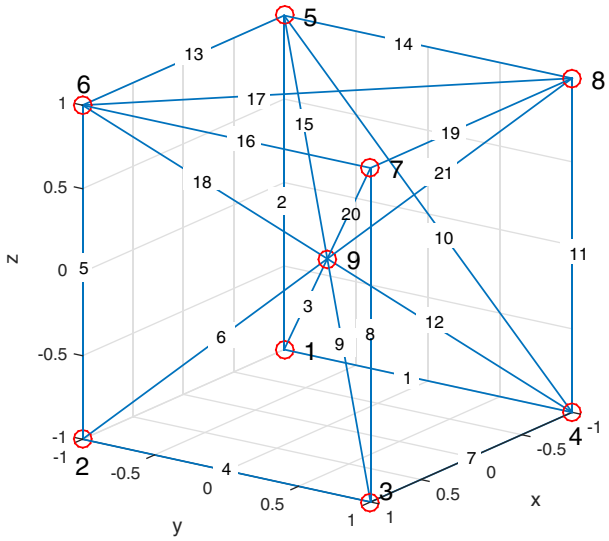

Fig. 3. Simulation 1: Desired formation F^d. [Color figure can be viewed at wileyonlinelibrary.com]

© 2018 Chinese Automatic Control Society and John Wiley & Sons Australia, Ltd

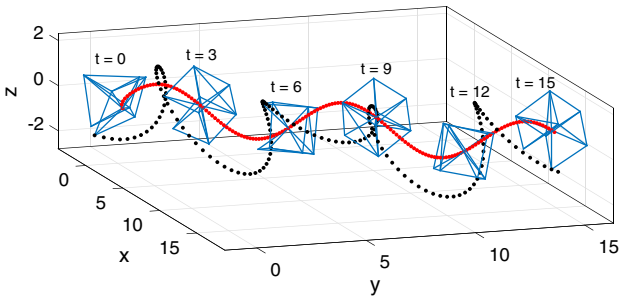

Fig. 4. Simulation 1: Snapshots in time of the formation maneuver. Black markers are the trajectory of agent 2; red line is the trajectory of the leader agent. [Color figure can be viewed at wileyonlinelibrary.com]

with edge length of 2 shown in Fig. 3. For ease of implementation, the eight vertices of the cube were chosen to represent the followers while the geometric center of the cube (point $[0,0,0]$) was chosen to represent the leader (*i.e.*, agent 9); thus, $V^d = \{1,\dots,9\}$. The required MR and IR condition of F^d was enforced by introducing 21 ($= 3\times 9 - 6$) edges with all followers connected to the leader. Therefore, from the ordering of edges shown in Fig. 3, the edge set became $E^d = \{(1,4),\ (1,5),\ (1,9),\dots,(7,9),\ (8,9)\}$.

The desired inter-agent distances were given by $d_{14} = d_{15} = d_{23} = d_{26} = d_{34} = d_{37} = d_{48} = d_{56} = d_{58} = d_{67} = d_{78} = 2$, $d_{19} = d_{29} = d_{39} = d_{49} = d_{59} = d_{69} = d_{79} = d_{89} = \sqrt{3}$, and $d_{45} = d_{68} = 2\sqrt{2}$. The initial condition for the ith agent, $q_i(0)$, was selected by randomly perturbing the corresponding value of q_i^* in Fig. 3.

The translation and angular velocities in (27) were chosen as

$$v_0 = [1, 1, \cos t]^\top \quad \text{and} \quad \omega_0 = [1,1,1]^\top, \tag{36}$$

which results in a screw-like motion for the formation. The control gain k_s in (26) was set to 0.3. Fig. 4 depicts snapshots of the actual formation $F(t)$ over time. As the agents acquire the desired formation by $t = 3$, they maneuver as a rigid body according to (27) and (36). Fig. 5 shows the distance errors $e_{ij}(t)$, $(i,j) \in E^d$ converging to zero, confirming that (13) is indeed satisfied. The components of each agent control input along the x-, y- and z-directions are shown in Fig. 6. The velocity-level control signals converge to (27) and (36) as expected according to (14). Specifically, notice that the x and y components are offset by 1 while, in the z direction, the signals have a lower frequency component with period 2π that results from $\cos t$ in (36).

Simulation 2. Since the single-integrator equation (11) is a simplified agent model, we considered in this second simulation a more realistic model in the form of unicycle vehicles moving on the plane. Fig. 7 depicts the ith vehicle, where the reference frame $\{X_0, Y_0\}$ is fixed to the Earth. The moving reference frame $\{X_i, Y_i\}$ is attached to the ith vehicle with the X_i

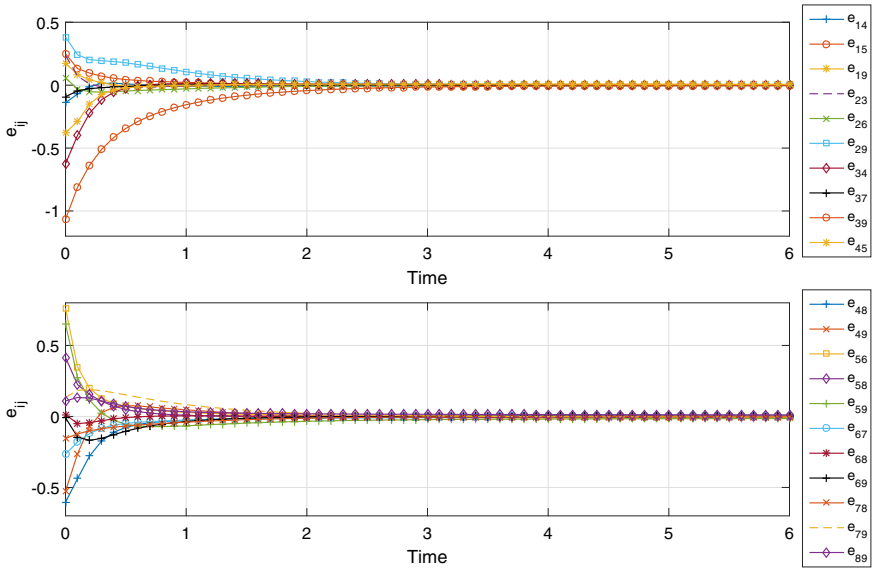

Fig. 5. Simulation 1: Distance errors $e_{ij}(t)$, $(i,j) \in E^d$. [Color figure can be viewed at wileyonlinelibrary.com]

© 2018 Chinese Automatic Control Society and John Wiley & Sons Australia, Ltd

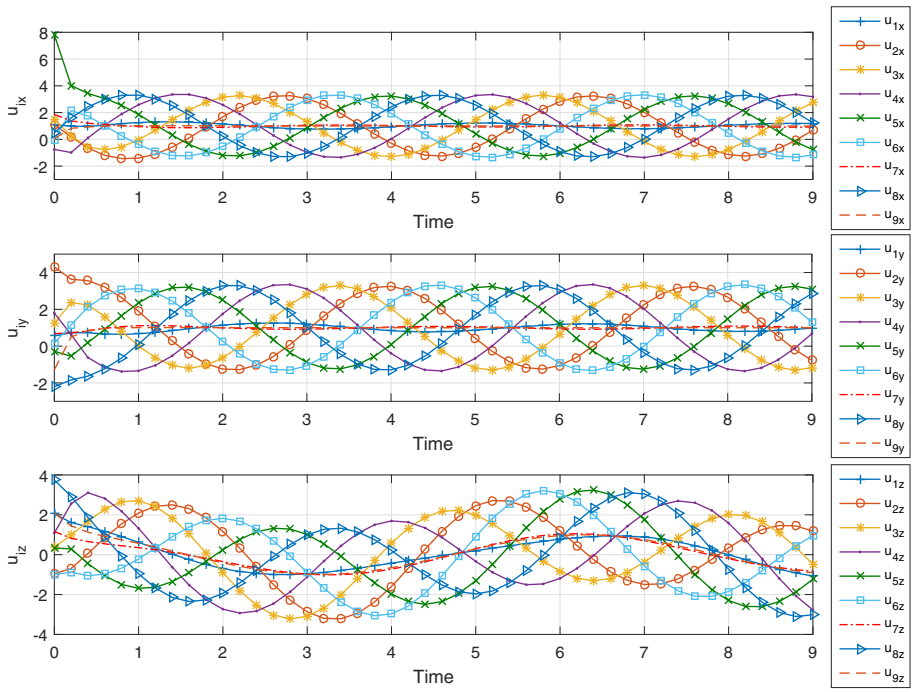

Fig. 6. Simulation 1: Control inputs $u_i(t)$, $i \in V^d$ in the x, y, and z directions. [Color figure can be viewed at wileyonlinelibrary.com]

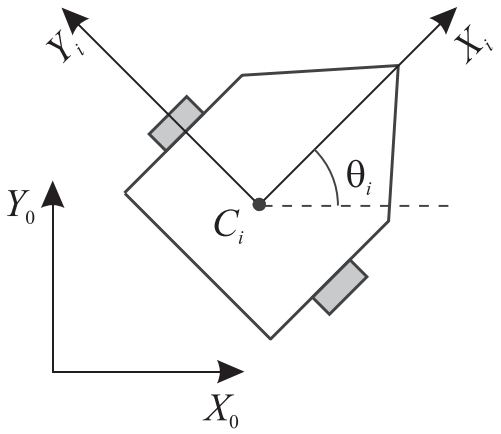

Fig. 7. Top view of the unicycle agent.

axis aligned with its heading (longitudinal) direction, which is given by angle θ_i and measured counterclockwise from the X_0 axis. Point C_i denotes the ith vehicle's center of mass which is assumed to coincide with its center of rotation.

The unicycle motion is governed by the following nonholonomic kinematic equation

$$\dot{q}_i = S(\theta_i)\eta_i, \quad i = 1, \ldots, n. \tag{37}$$

where $q_i = [x_i, y_i, \theta_i]^\top$ denotes the position and orientation of $\{X_i, Y_i\}$ relative to $\{X_0, Y_0\}$, $\eta_i = [v_i, \omega_i]$ is the control input, v_i is the ith agent's translational speed in the direction of θ_i, ω_i is the ith agent's angular speed about the vertical axis passing through C_i, and

$$S(\theta_i) = \begin{bmatrix} \cos\theta_i & 0 \\ \sin\theta_i & 0 \\ 0 & 1 \end{bmatrix}. \tag{38}$$

In order to apply (26) to (37), we introduce the input transformation

$$v_i = u_{ix}\cos\theta_i + u_{iy}\sin\theta_i \tag{39a}$$

$$\omega_i = -\alpha_i\tilde{\theta}_i \tag{39b}$$

where $u_i = [u_{ix}, u_{iy}]^\top$ is given by (35), $\alpha_i > 0$ is a control gain, $\tilde{\theta}_i = \theta_i - \theta_{di}$, and

$$\theta_{di} = \begin{cases} 0, & \text{if } u_{ix} = u_{iy} = 0 \\ \operatorname{atan2}(u_{iy}, u_{ix}), & \text{otherwise.} \end{cases} \tag{40}$$

In this simulation, the desired formation F^d was set to the regular pentagon shown in Fig. 8. Vehicle 6 was selected as the leader, and nine edges were introduced to ensure F^d was IR and MR. The desired inter-agents distances were $d_{i6} = 0.1$, $i = 1, \ldots, 5$ and

© 2018 Chinese Automatic Control Society and John Wiley & Sons Australia, Ltd

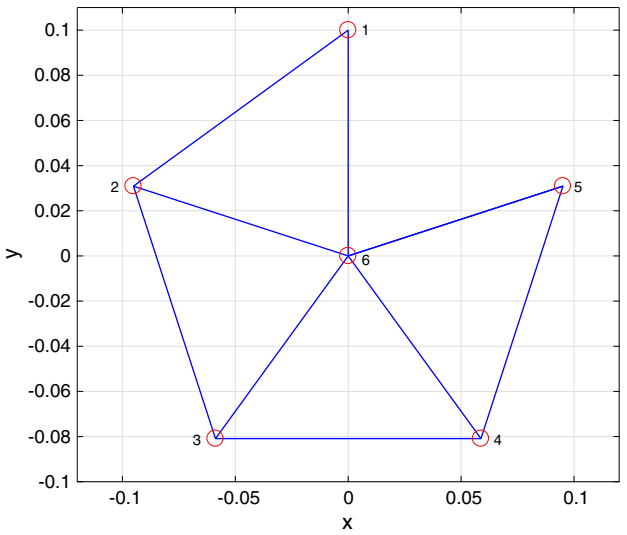

Fig. 8. Simulation 2: Desired formation F^d. [Color figure can be viewed at wileyonlinelibrary.com]

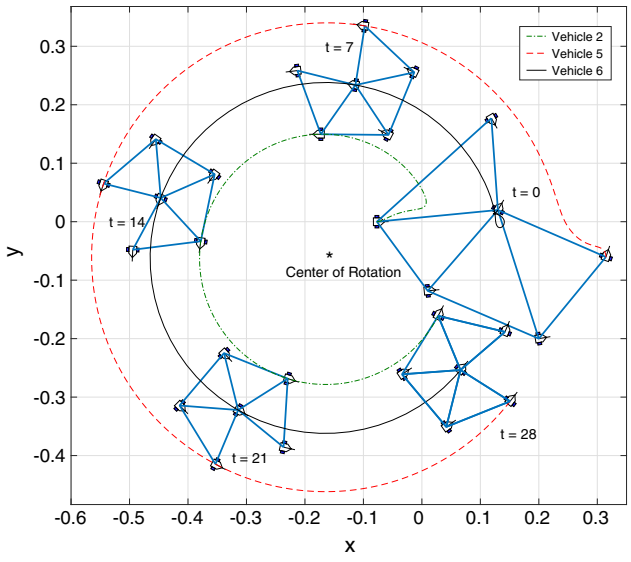

Fig. 9. Simulation 2: Snapshots in time of the formation maneuver. [Color figure can be viewed at wileyonlinelibrary.com]

$d_{12} = d_{23} = d_{34} = d_{45} = 0.1176$. The translation and angular velocities were set to

$$v_0 = \left[-6\sin 0.2t,\ 6\cos 0.2t,\ 0\right]^\top \times 10^{-2} \quad \text{and}$$
$$\omega_0 = [0, 0, 0.2]^\top,$$

which correspond to a circular orbit of the formation about the z-axis with Vehicle 2 always located in the interior of the orbit. The control gains were set to $k_s = 50$ in (26) and $\alpha_i = 20$, $i = 1, \ldots, 6$ in (39b). We also considered that the control inputs are constrained by $|v_i| \leq 0.1$ and $|\omega_i| \leq 2\pi$ since actual robotic vehicles have limits on their actuation commands.

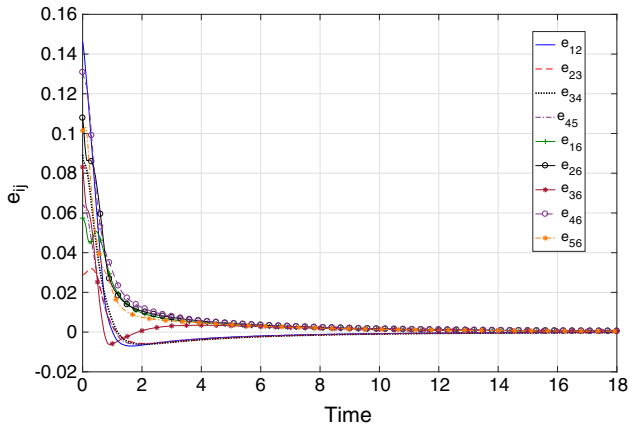

Fig. 10. Simulation 2: Distance errors $e_{ij}(t)$, $(i,j) \in E^d$. [Color figure can be viewed at wileyonlinelibrary.com]

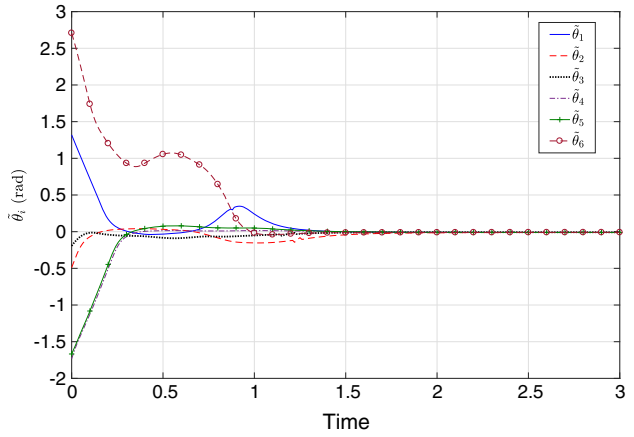

Fig. 11. Simulation 2: Heading angle error $\tilde{\theta}(t)$, $i \in V^d$. [Color figure can be viewed at wileyonlinelibrary.com]

Fig. 9 shows snapshots of the formation maneuver along with the trajectory of three of the vehicles for illustration purposes. The distance errors are shown in Fig. 10, indicating that the formation is accurately acquired at about $t = 15$. The heading angle errors $\tilde{\theta}_i(t)$ of each vehicle are depicted in Fig. 11, and show that the simple proportional control in (39b) is effective in tracking the desired heading angle. Finally, the control inputs are shown in Fig. 12, where one can see that saturation only occurs during a brief transient period.

© 2018 Chinese Automatic Control Society and John Wiley & Sons Australia, Ltd

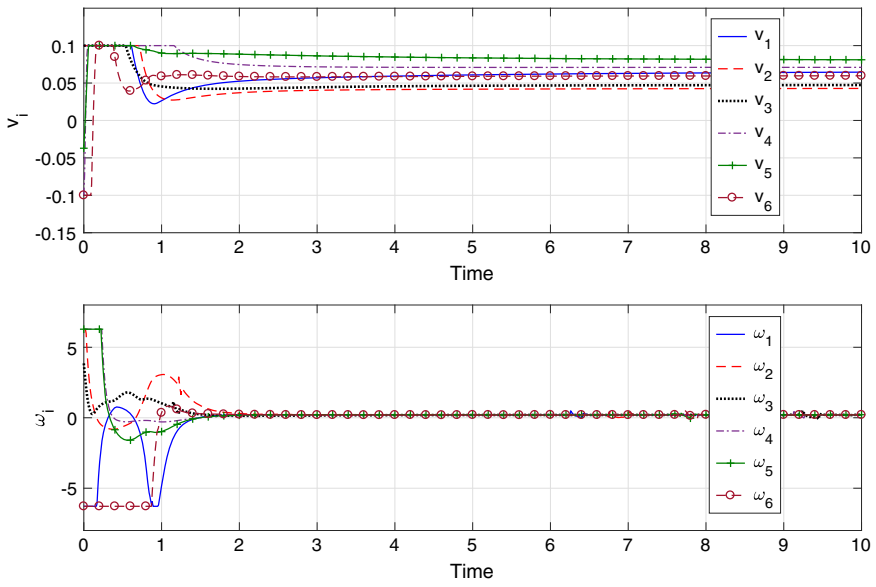

Fig. 12. Simulation 2: Control inputs $v_i(t)$ and $\omega_i(t)$, $i \in V^d$. [Color figure can be viewed at wileyonlinelibrary.com]

VI. CONCLUSIONS

This paper presented a formation controller that permits the multi-agent formation to maneuver as a virtual rigid body in space while ensuring the stabilization of the inter-agent distance dynamics. A leader-follower type scheme was used to facilitate the specification of the desired rigid body motion. The proposed control law only needs the relative position of agents linked in the infinitesimally and minimally rigid graph to be sensed. The exponential stability of the distance error dynamics and the tracking of the desired rigid body maneuver were proven via Lyapunov theory for the single-integrator model. As is common to formation controllers based on inter-agent distance control, the stability properties of the proposed formation maneuvering control are only local in nature. That is, the formation may converge to an ambiguous framework for initial conditions outside of the set given in Theorem 1.

REFERENCES

1. Anderson, B. D. O., C. Yu, B. Fidan, and J. M. Hendrickx, "Rigid graph control architectures for autonomous formations," *IEEE Control Syst. Mag.*, Vol. 28, No. 6, pp. 48–63 (2008).
2. Asimow, L. and B. Roth, "The rigidity of graphs II," *J. Math. Anal. Appl.*, Vol. 68, No. 1, pp. 171–190 (1979).
3. Aspnes, J., J. Egen, D. K. Goldenberg, A. S. Morse, W. Whiteley, Y. R. Yang, B. D. O. Anderson, and P. N. Belhumeur, "A theory of network localization," *IEEE Trans. Mob. Comput.*, Vol. 5, No. 12, pp. 1663–1678 (2006).
4. Bai, H., M. Arcak, and J. T. Wen, "Using orientation agreement to achieve planar rigid formation," *Proc. Amer. Control Conf.*, Seattle, WA, pp. 753–758 (2008).
5. Beer, F. P., E. R. Johnston, and W. E. Clausen, *Vector Mechanics for Engineers: Dynamics*, Mcgraw Hill, New York, NY (2007).
6. Cai, X. and M. de Queiroz, "Multi-agent formation maneuvering and target interception with double-integrator model," *Proc. Amer. Control Conf.*, Portland, OR, pp. 287–292 (2014).
7. Cai, X and M. de Queiroz, "Rigidity-based stabilization of multi-agent formations," *SME J. Dyn. Syst. Meas. Control*, Vol. 136, No. 1, pp. 014502 (2014).
8. Cai, X. and M. de Queiroz, "Adaptive rigidity-based formation control for multi-robotic vehicles with dynamics," *IEEE Trans. Control Syst. Tech.*, Vol. 23, No. 1, pp. 389–396 (2015).
9. Cai, X. and M. de Queiroz, "Formation maneuvering and target interception for multi-agent systems via rigid graphs," *Asian J. Control*, Vol. 17, No. 4, pp. 1174–1186 (2015).
10. Cao, M., A. S. Morse, C. Yu, B. D. O. Anderson, and S. Dasgupta, "Maintaining a directed, triangular

© 2018 Chinese Automatic Control Society and John Wiley & Sons Australia, Ltd

formation of mobile autonomous agents," *Commun. Inf. Syst.*, Vol. 11, No. 1, pp. 1–16 (2011).
11. Cheng, L., Y. Wang, W. Ren, Z.-G. Hou, and M. Tan, "Containment control of multiagent systems with dynamic leaders based on PI^n-type approach," *IEEE T. Cybern.*, Vol. 46, No. 12, pp. 3004–3017 (2016).
12. Connelly, R., "Generic global rigidity," *Discrete Comput. Geom.*, Vol. 33, No. 4, pp. 549–563 (2005).
13. de Marina, H. G., B. Jayawardhana, and M. Cao, "Distributed rotational and translational maneuvering of rigid formations and their applications," *IEEE Trans. Robot.*, Vol. 32, No. 3, pp. 684–697 (2016).
14. Dong, X., B. Yu, Z. Shi, and Y. Zhong, "Time-varying formation control for unmanned aerial vehicles: theories and applications," *IEEE Trans. Control Syst. Tech.*, Vol. 23, No. 1, pp. 340–348 (2015).
15. Dörfler, F. and B. Francis, "Geometric analysis of the formation problem for autonomous robots," *IEEE Trans. Autom. Control*, Vol. 55, No. 10, pp. 2379–2384 (2010).
16. Eren, T., P. N. Belhumeur, B. D. O. Anderson, and A. S. Morse, "A framework for maintaining formations based on rigidity," *Proc. IFAC Congr.*, Barcelona, Spain, pp. 2752–2757 (2002).
17. Gazi, V. and B. Fidan, "Adaptive formation control and target tracking in a class of multi-agent systems: Formation maneuvers," *Int. Conf. Control Autom. Syst.*, Gwangju, Korea, pp. 78–85 (2013).
18. Gazi, V. and K. M. Passino, *Swarm Stability and Optimization*, Springer, Berlin (2011).
19. Gutiérrez, H., A. Morales, and H. Nijmeijer, "Synchronization control for a swarm of unicycle robots: Analysis of different controller topologies," *Asian J. Control*, Vol. 19, No. 6, pp. 1–12 (2017).
20. Han, T., M. Chi, Z.-H. Guan, B. Hu, J.-W. Xiao, and Y. Huang, "Distributed three-dimensional formation containment control of multiple unmanned aerial vehicle systems," *Asian J. Control*, Vol. 19, No. 3, pp. 1103–1113 (2017).
21. Han, Z., L. Wang, Z. Lin, and R. Zheng, "Formation control with size scaling via a complex laplacian-based approach," *IEEE T. Cybern.*, Vol. 46, No. 10, pp. 2348–2359 (2016).
22. "Special issue on collective behavior and control of multi-agent systems," *Asian J. Control*, Vol. 10, No. 2, pp. 129–130 (2008).
23. Izmestiev, I., *Infinitesimal Rigidity of Frameworks and Surfaces*, Lectures on Infinitesimal Rigidity, Kyushu University, Japan (2009).
24. Jackson, B., "Notes on the rigidity of graphs," *Levico Conference Notes*, Levico Terme, Italy (2007).
25. Khalil, H. K., *Nonlinear Systems*, Prentice Hall, Englewood Cliffs, NJ (2002).
26. Krick, L., M. E. Broucke, and B. A. Francis, "Stabilization of infinitesimally rigid formations of multi-robot networks," *Int. J. Control*, Vol. 83, No. 3, pp. 423–439 (2009).
27. Liu, Y., Y. Zhao, and G. Chen, "Finite-time formation tracking control for multiple vehicles: A motion planning approach," *Int. J. Robust Nonlinear Control*, Vol. 26, No. 14, pp. 3130–3149 (2016).
28. Meng, D., Y. Jia, J. Du, and F. Yu, "Tracking control over a finite interval for multi-agent systems with a time-varying reference trajectory," *Syst. Control Lett.*, Vol. 61, No. 7, pp. 807–818 (2012).
29. Niu, X., Y. Liu, and Y. Man, "Adaptive leader-following consensus for uncertain nonlinear multi-agent systems," *Asian J. Control*, Vol. 19, No. 3, pp. 1189–1196 (2017).
30. Oh, K.-K. and H.-S. Ahn, "Distance-based control of cycle-free persistent formations," *Proc. IEEE Multi-Conf. Syst. Control*, Denver, CO, pp. 816–821 (2011).
31. Oh, K.-K. and H.-S. Ahn, "Distance-based undirected formations of single-integrator and double-integrator modeled agents in n-dimensional space," *Int. J. Robust Nonlinear Control*, Vol. 24, No. 12, pp. 1809–1820 (2014).
32. Oh, K.-K. and H.-S. Ahn, "Formation control of mobile agents based on inter-agent distance dynamics," *Automatica*, Vol. 47, No. 10, pp. 2306–2312 (2011).
33. Ramazani, S., R. Selmic, and M. de Queiroz, "Rigidity-based multiagent layered formation control," *IEEE T. Cybern.*, Vol. 47, No. 8, pp. 1902–1913 (2017).
34. Ren, W. and Y. Cao, *Distributed Coordination of Multi-Agent Networks: Emergent Problems, Models, and Issues*, Springer-Verlag, London (2011).
35. Rozenheck, O., S. Zhao, and D. Zelazo, "A proportional-integral controller for distance based formation tracking," *Proc. Eur. Control Conf.*, Linz, Austria, pp. 1693–1698 (2015).
36. Summers, T. H., C. Yu, S. Dasgupta, and B. D. O. Anderson, "Control of minimally persistent leader-remote-follower and coleader formations in the plane," *IEEE Trans. Autom. Control*, Vol. 56, No. 12, pp. 2778–2792 (2011).
37. Wang, L., J. Markdahl, and X. Hu, "Distributed attitude control of multi-agent formations," *Proc. IFAC World Cong.*, Milan, Italy, pp. 2965–2971 (2011).
38. Zhao, Y., Z. Duan, G. Wen, and G. Chen, "Distributed finite-time tracking of multiple non-identical second-order nonlinear systems with

© 2018 Chinese Automatic Control Society and John Wiley & Sons Australia, Ltd

settling time estimation," *Automatica*, Vol. 64, pp. 86–93 (2016).
39. Zhao, Y., Y. Liu, Z. Li, and Z. Duan, "Distributed average tracking for multiple signals generated by linear dynamical systems: an edge-based framework," *Automatica*, Vol. 75, pp. 158–166 (2017).
40. Zhao, Y., Y. Liu, G. Wen, and G. Chen, "Distributed optimization of linear multi-agent systems: Edge- and node-based adaptive designs," *IEEE Trans. Autom. Control*, Vol. 62, No. 7, pp. 3602–3609 (2017).

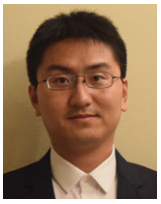

Pengpeng Zhang received a B.S. degree in Mechanical Engineering from Shandong University, Jinan, Shandong, China, in 2013. He is currently working toward his Ph.D. degree in Mechanical Engineering under the supervision of Dr. Marcio de Queiroz at Louisiana State University, United States. His main research interest is formation control of multi-agent systems.

Marcio de Queiroz received a B.S. Degree in Electrical Engineering from the Federal University of Rio de Janeiro, Brazil, a M.S. Degree in Mechanical Engineering from the Pontifical Catholic University of Rio de Janeiro, Brazil, and a Ph.D. Degree in Electrical Engineering from Clemson University, Clemson, SC in 1997. From August 1997 to August 1998 he was a Post-Doctoral Researcher at the Rotating Machinery and Controls Laboratories of the University of Virginia. From September 1998 to May 2000, he was a Visiting Assistant Professor at the Department of Mechanical Engineering of the NYU Tandon School of Engineering. In July 2000, he joined the Department of Mechanical and Industrial Engineering at LSU, where he is currently the Roy O. Martin Lumber Company Professor. In 2005, he was the recipient of the NSF CAREER award. Dr. Queiroz served as an Associate Editor for the IEEE Transactions on Automatic Control, the ASME Journal of Dynamic Systems, Measurement, and Control, the IEEE/ASME Transactions on Mechatronics, and the IEEE Transactions on Systems, Man, and Cybernetics Part B. He is currently the coordinator for the Robotics Engineering minor for the LSU College of Engineering. His research interests include nonlinear control theory and applications, multi-agent systems, robotics, active magnetic and mechanical bearings, and biological/biomedical system modeling and control.

© 2018 Chinese Automatic Control Society and John Wiley & Sons Australia, Ltd